

ABSOLUTE VACUUM ULTRAVIOLET OSCILLATOR STRENGTHS IN Co II AND THE INTERSTELLAR COBALT ABUNDANCE¹

K. L. MULLMAN AND J. E. LAWLER

Department of Physics, University of Wisconsin at Madison, Madison, WI 53706

AND

J. ZSARGÓ AND S. R. FEDERMAN

Department of Physics and Astronomy, University of Toledo, Toledo, OH 43606

Received 1997 December 5; accepted 1998 January 26

ABSTRACT

We report the first laboratory measurements of 10 absolute oscillator strengths (f -values) for vacuum ultraviolet lines of Co II. The oscillator strengths are measured with the High-Sensitivity Absorption Spectroscopy Experiment at the University of Wisconsin. The measurements serve as a test of theoretical work on Co II f -values and set an absolute scale for relative oscillator strengths from spectra taken with the *Hubble Space Telescope*. Observations of interstellar absorption in the direction of ρ Oph A result in the determination of the f -value for an additional line. The set of absolute f -values is used to derive the interstellar abundance of cobalt toward ρ Oph A and ζ Oph. Cobalt is found to be less severely depleted onto grains than earlier analyses based on available theoretical f -values suggested. As a consequence of this revision, the correspondence between depletion and condensation temperature is somewhat weakened.

Subject headings: atomic data — ISM: abundances — methods: laboratory — ultraviolet: ISM

1. INTRODUCTION

In order to determine accurate abundances and depletions in stars and interstellar material, accurate oscillator strengths (f -values) are required. With the launch of orbiting observatories such as the *Hubble Space Telescope* (*HST*), which routinely provide high-quality data at short wavelengths, these needs have become more urgent, especially in the vacuum ultraviolet (VUV). Singly ionized cobalt is seen in a wide variety of objects, including OB type stars, the interstellar medium, and QSO absorption-line clouds (Shull 1993). Because Co II is not as abundant as common species such as Fe II or Si II, it can be used to determine accurate abundances for “nucleosynthetic products from stars other than those producing the CNO group and Si/S group” (Shull 1993). Weaker lines are also useful along lines of sight where the stronger transitions are saturated and no longer give accurate abundances.

We report the first laboratory measurements of absolute f -values for 10 VUV transitions in Co II with $146.621 \text{ nm} \leq \lambda_{\text{vac}} \leq 195.743 \text{ nm}$. These measurements were made with the High-Sensitivity Absorption Spectroscopy Experiment at the University of Wisconsin (Bergeson, Mullman, & Lawler 1996). The experiment uses the Aladdin storage ring at the Synchrotron Radiation Center as a continuum source, a hollow cathode discharge (HCD) as an absorbing sample, and a 3 m focal length vacuum echelle spectrometer equipped with a CCD detector array. Although we are reporting work done on Co II, this experiment is applicable to essentially every element of the periodic table, both neutral and singly ionized species, over a wide range of wavelength and line strengths. Because the HCD is not in LTE, the absorption experiment yields relative f -values of lines from a common lower level. The absolute scale for

these measurements was determined by combining branching fraction measurements made on our 3 m spectrometer with radiative lifetimes measured using laser-induced fluorescence (Mullman, Cooper, & Lawler 1998).

Our spectra of interstellar gas toward ρ Oph A, acquired with the Goddard High-Resolution Spectrograph (GHRS) on *HST*, revealed three lines from Co II, two of which were studied in the experiment reported here. This allows us to place the f -value for the line at $\lambda_{\text{vac}} = 144.801 \text{ nm}$ on an absolute scale as well. The combined set of absolute f -values for 11 Co II lines provides the basis for determining the Co II abundance in the gas toward ρ Oph A and ζ Oph. Since Co II is the dominant ion for this material, we also present the first accurate abundances for interstellar cobalt, which are useful in studies of the evolution of interstellar grains.

2. LABORATORY ABSORPTION MEASUREMENTS

A classic absorption experiment requires three components: a continuum source, an absorbing sample, and a spectrometer/detector system. A schematic of the apparatus can be found in Bergeson et al. (1996). Our continuum source is the white light beam line on the Aladdin Storage Ring at the Synchrotron Radiation Center. The synchrotron provides a bright, smooth, stable continuum over the entire UV and VUV wavelength ranges. Typical operating parameters of the electron storage ring are 800 MeV beam energy, 200 mA initial stored current, and a 2.083 magnetic bending radius. Our 1 cm inner diameter, 10 cm (or 20 cm) long, water-cooled HCD provides a low-pressure, gas-phase sample of Co atoms and ions. Both the neutral atom and the singly ionized species have useful populations for absorption from the ground level and many of the lower metastable levels. Typical operating parameters for the HCD include 1.3 torr of Ar buffer gas and currents ranging from 300 to 700 mA.

Our spectrometer/detector system is a 3 m focal length vacuum-compatible echelle spectrograph equipped with a VUV-sensitive CCD detector array. The CCD is a Scientific

¹ Based on observations obtained with the NASA/ESA *Hubble Space Telescope* through the Space Telescope Science Institute, which is operated by the Association of Universities for Research in Astronomy, Inc., under NASA contract NAS 5-26555.

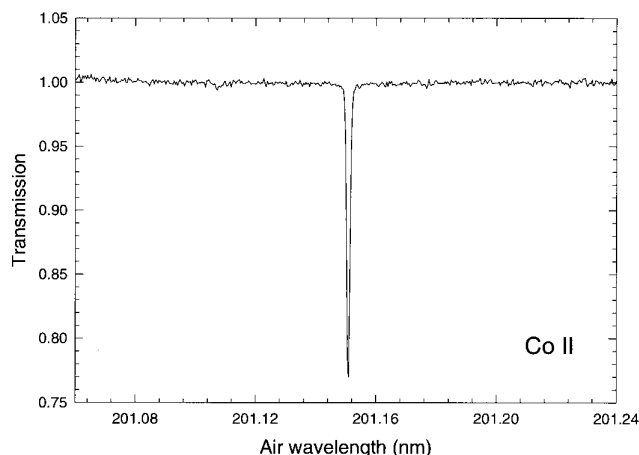


FIG. 1.—Absorption at $\lambda_{\text{air}} = 201.151$ nm in Co II. The noise in the continuum is consistent with Poisson statistics of the photoelectrons in the CCD array.

Imaging Technologies uncoated, boron-doped, thinned, back-illuminated, VUV-sensitive device in a camera head from Princeton Instruments. The CCD format is square, with 512 pixels on a side. With the 256 mm wide, 63° blaze echelle grating, the practical resolving power of this system is $\sim 350,000$. Because the spectrometer operates between 28th and 40th order for these measurements, a McPherson model 234/304 Seya premonochromator is used as an order sorter. To reduce stray light in the spectrometer, we limit the Seya bandpass to 0.3 nm. Figures 1 and 2 show the high signal-to-noise ratio of our data in the UV and VUV, respectively. The noise in the continuum of both figures is equivalent to Poisson statistical noise for the photoelectrons. This experiment is now sensitive to fractional absorptions much smaller than 1%; column densities as small as $3 \times 10^8 \text{ cm}^{-2}$ have been detected for neutral atoms and atomic ions in both the UV and VUV wavelength ranges. Substantial further improvements in sensitivity are planned.

The shape of the synchrotron beam is carefully set with several cylindrical mirrors to match the angular acceptance of the spectrometer; the optical coupling is described in

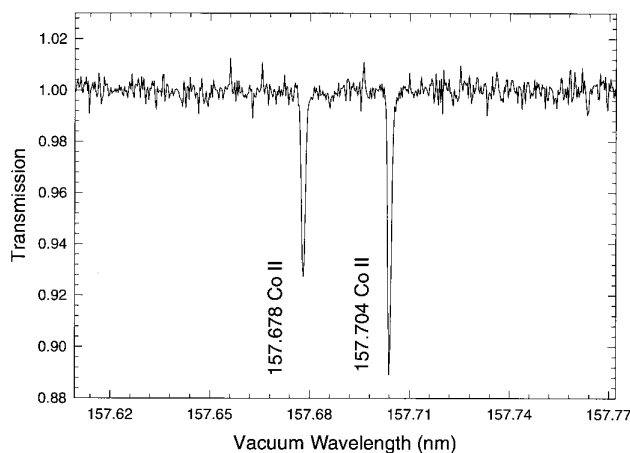


FIG. 2.—Sample spectrum of absorption at $\lambda_{\text{vac}} = 157.7$ nm in Co II. The noise in the continuum is consistent with Poisson statistics of the photoelectrons in the CCD array.

detail elsewhere (Bergeson et. al. 1996). The *étendue* of the reshaped synchrotron beam is a rather good match to the *étendue* of the 3 m echelle spectrometer. The synchrotron beam does not have a large enough *étendue* to fill a typical Fourier Transform Spectrometer (FTS). The lack of a usable *étendue* advantage, along with a signal-to-noise disadvantage from the spectral redistribution of quantum (Poisson) noise intrinsic to the FTS, means that an FTS does not have an advantage over a grating spectrometer in this type of experiment.

We use a digital subtraction technique to discriminate against line emission in the HCD (Wamsley, Mitsuhashi, & Lawler 1993). With the synchrotron continuum passing through our sample, the spectrum is a combination of the synchrotron continuum, absorption from atoms and ions in the line of sight, emission from the HCD, and dark signal from the array. By blocking the synchrotron, we get a spectrum of only the HCD emission plus the dark signal. The subtraction of these two spectra results in the continuum plus absorption spectrum. Pixel-to-pixel variations in the quantum efficiency of the detector can be taken into account by dividing the difference spectrum described above by a dark signal corrected, high signal-to-noise continuum spectrum taken with the HCD off.

When using this digital subtraction technique, the linearity of the detector array is especially important (Menningen et. al. 1995). We measure the fractional nonlinearity of our CCD array and find it to be less than 0.001 from 4% full-well to 85% full-well. We have designed our optical coupling so that the HCD line emission is much less than the synchrotron continuum. In this situation, the small nonlinearities of the detector have no effect on our absorption signal.

Scattered light can cause an error in absorption measurements; we have taken special care to measure the scattered light in our system by completing a separate absorption experiment. When the column density is high in an absorbing sample, the observed absorption feature is completely saturated. Measuring the light level at line center under these conditions provides a direct measurement of the scattered light in our system. We place a Hg vapor cell in the line of sight and measure absorption at the 254 nm resonance line. We also did absorption measurements at 190 nm and 147 nm by filling the HCD chamber with O_2 and Xe gas, respectively. All of these measurements show that the scattered light level in our system is $\leq 2\%$ when the bandpass of the Seya premonochromator is limited to 0.2 nm or less. For the 2 lines with $\lambda_{\text{vac}} \leq 149$ nm, the Seya bandpass was increased to 0.8 nm to avoid unreasonably long integration times. The scattered light at this bandpass and wavelength is measured by repeating the Xe absorption experiment. The scattered light is 18% with the increased bandpass; the increased scattered light is included in the analysis of data taken on these 2 lines.

In an absorption experiment, it is important to verify that the measurements are made on the linear part of the curve of growth or that the data is analyzed properly, using a nonlinear curve of growth. We have verified that we are making measurements on or very near the linear part of the curve of growth by measuring ratios of well-known reference lines at each of the currents used in the experiment. The f -values of the reference lines were determined by combining branching fraction measurements with laser-induced fluorescence lifetime measurements (Mullman et. al. 1998).

TABLE 1
WELL-KNOWN ABSORPTION OSCILLATOR STRENGTH RATIOS FOR CO II LINES AND
ABSORPTION RESULTS

$(\lambda_1/\lambda_2)_{\text{air}}$ (nm)	$(f_1/f_2)^a$	HOLLOW CATHODE DISCHARGE CURRENT (A)				
		0.50	0.55	0.60	0.65	0.70
201.151/205.882.....	4.9(6)	5.4(2)	6.0(4)	5.7(2)	5.6(2)	5.93(11)
202.576/205.882.....	1.7(3)	1.76(14)	1.82(9)	2.0(2)	1.71(12)	1.94(10)
201.151/202.576.....	3.0(4)	3.8(2)	3.78(11)	3.25(15)	3.65(19)	3.42(18)
202.235/206.554.....	3.9(6)	3.8(3)	4.16(13)	4.0(3)	4.03(13)	4.0(3)

NOTE.—Line pairs listed have a common lower level. The absorption results are shown for each hollow cathode discharge current used in this experiment. The numbers in parentheses after each entry designate the uncertainty in the last digit(s) of the entry.

^a Oscillator strengths from emission-branching fraction measurements and laser-induced fluorescence lifetime measurements (Mullman et. al. 1998).

These are the same reference lines that are used to set the absolute scale for the VUV f -value measurements reported here. Table 1 verifies that the absorption results agree with the emission results within the uncertainties of both experiments. This demonstrates that the HCD operates on the linear part of the curve of growth for the currents used in this experiment. In order to be as accurate as possible, we have included a small curve-of-growth correction into our data analysis. Since the HCD is operating very close to the linear portion of the curve of growth, we assume a Doppler line shape and make a correction to the data that includes the first nonlinear term in the curve of growth. For most of the transitions, this correction is much less than 5%, but for a few of the stronger lines at high-discharge currents, the correction is as large as 10%. The data in both tables includes this small curve-of-growth correction.

3. LABORATORY RESULTS

We measure 10 VUV lines of Co II to an accuracy better than $\pm 10\%$. Each transition was measured relative to two different UV transitions. This provides us with an internal consistency check for our data, since we know accurate f -values for each of the UV transitions used as reference lines in this experiment. For example, the transition at $\lambda_{\text{vac}} = 155.275$ nm was measured relative to both

$\lambda_{\text{air}} = 201.151$ nm and $\lambda_{\text{air}} = 202.576$ nm. We find $f(\lambda_{\text{air}} = 201.151)/f(\lambda_{\text{vac}} = 155.275) = 3.27(17)$ and $f(\lambda_{\text{air}} = 202.576)/f(\lambda_{\text{vac}} = 155.275) = 1.03(5)$, where f is the absorption oscillator strength. From the emission work, we know $f(\lambda_{\text{air}} = 201.151)/f(\lambda_{\text{air}} = 202.576) = 3.0(4)$. From the absorption work, we find $f(\lambda_{\text{air}} = 201.151)/f(\lambda_{\text{air}} = 202.576) = [f(\lambda_{\text{air}} = 201.151)/f(\lambda_{\text{vac}} = 155.275)]/[f(\lambda_{\text{air}} = 202.576)/f(\lambda_{\text{vac}} = 155.275)] = 3.2(2)$, which agrees very well with the emission result. This cross check allowed us to identify inconsistencies in our data set. For the a^3F_2 lower level, we have only one reference line ($\lambda_{\text{air}} = 202.705$ nm) that has been studied in emission. We identified another line connected to that lower level at $\lambda_{\text{air}} = 206.379$ nm and adopted it as our second reference line. We measured the ratio $f(\lambda_{\text{air}} = 202.705)/f(\lambda_{\text{air}} = 206.379)$ in absorption and used that result to check the VUV measurements for transitions from the a^3F_2 level.

The first entries in Table 2 are the absolute VUV f -values measured here. All of the transitions are connected to the ground term. Energy levels in the tables are from Sugar & Corliss (1985); wavelengths are from Iglesias (1979). New, more accurate energy levels are in a recently submitted manuscript (Pickering et. al. 1998). As mentioned earlier, the f -values have typical accuracies of 10%. These accuracies are limited in part by the uncertainties on the UV

TABLE 2
ABSOLUTE ABSORPTION OSCILLATOR STRENGTHS FOR VUV TRANSITIONS IN CO II.

λ_{vac} (nm)	LOWER LEVEL		UPPER LEVEL		f -VALUE	
	Term	E_l (cm^{-1})	Term	E_u (cm^{-1})	This work	Other results
195.743	a^3F_2	1597.32	$z^3D_0^o$	52684.77	0.033(3)	0.055 ^a , 0.028 ^b
195.009	a^3F_3	950.51	$z^3D_2^o$	52229.92	0.030(3)	0.066 ^a , 0.034 ^b
194.129	a^3F_4	0.00	$z^3D_3^o$	51512.41	0.034(3)	0.075 ^a , 0.039 ^b
157.704	a^3F_3	950.51	$y^3F_3^o$	64360.26	0.031(3)	0.081 ^a
157.678	a^3F_2	1597.32	$y^3F_2^o$	65017.06	0.057(6)	0.095 ^a
157.455	a^3F_4	0.00	$y^3F_4^o$	63510.40	0.025(2)	0.080 ^a
157.265	a^3F_4	0.00	$y^3D_3^o$	63587.01	0.0120(11)	0.025 ^a
155.275	a^3F_4	0.00	$z^1G_4^o$	64401.46	0.0116(9)	0.015 ^a
148.096	a^3F_4	0.00	$x^3D_3^o$	67524.20	0.0119(10)	0.046 ^a
146.621	a^3F_4	0.00	$x^3G_5^o$	68203.39	0.031(3)	0.140 ^a
144.801 ^c	a^3F_4	0.00	$w^3D_3^o$	69060.26	0.0079 $^{+0.0024}_{-0.0027}$	0.046 ^a

NOTE.—The numbers in parentheses after each entry designate the uncertainty in the last digit(s) of the entry.

^a Kurucz (1988).

^b Raassen et al. (1998).

^c Our astronomically derived f -value.

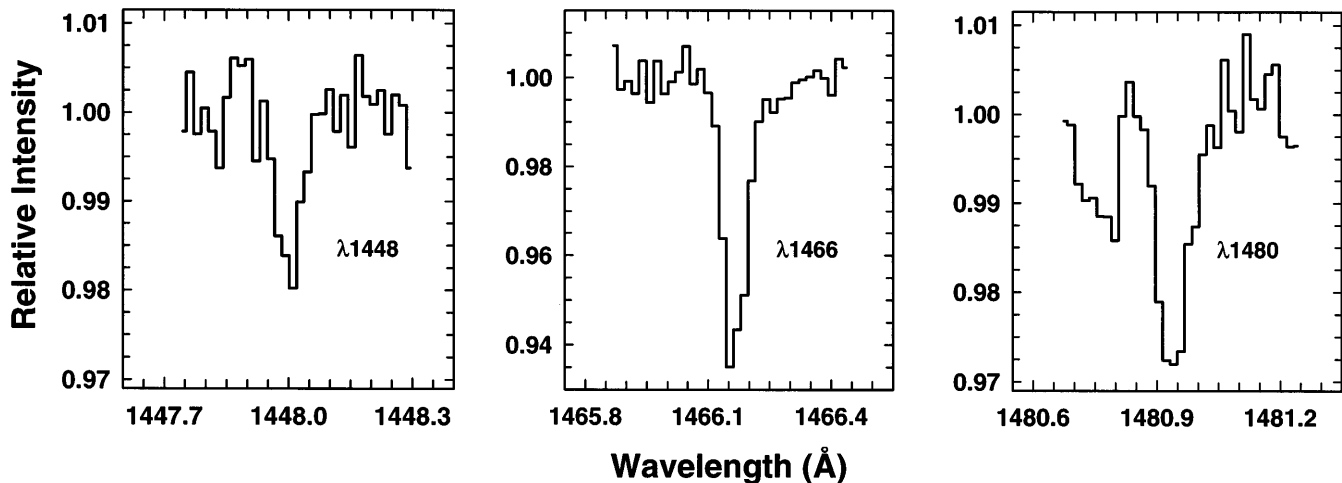


FIG. 3.—Co II lines seen in interstellar gas toward ρ Oph A. The vertical scale for $\lambda 1466$ is reduced by 50% compared to the other two panels.

reference lines. The f -values are compared to the theoretical results of Kurucz (1988) and Raassen, Pickering, & Ulyings (1998) in Table 2; the results of Kurucz (1988) were adopted by Morton (1991) for his compilation. The predictions of Raassen et al. (1998) are in very good agreement with our measurements. The theoretical predictions of Kurucz (1988) tend to be a factor of 2–3 larger than our experimental results; therefore, earlier analyses of the interstellar cobalt abundance (e.g., Federman et al. 1993) suggested abundances that were too low. In other words, there is less depletion of Co onto grains than once thought. This point is developed further in the next section.

4. ASTRONOMICAL RESULTS

Three absorption lines of Co II were detected from gas along the line of sight to ρ Oph A with the GHRS. The data sets were described previously in papers by Zsargó, Federman, & Cardelli (1997) and Zsargó & Federman (1998). Here we reiterate that special care was taken to minimize the effects of noise, thereby allowing detection of weak features. The three lines have laboratory wavelengths of 144.801, 146.621, and 148.096 nm. Figure 3 shows spectra containing the interstellar lines; note that the vertical scale for $\lambda 1466$ is reduced by 50%. Equivalent widths (W_λ), which appear in Table 3, were measured with NOAO's IRAF package. In addition to the usual uncertainty associated with the rms deviations in the stellar continuum, we derived systematic errors arising from continuum placement so that

a more meaningful comparison of relative line strengths for $\lambda\lambda 1466, 1480$ with experiment was possible. This was necessary because the interstellar line at 148.096 nm was on the shoulder of a stronger feature.

The analysis of the interstellar results proceeded in the following manner: The first step in extracting f -values from the astronomical data involved use of a curve of growth to derive the column density, N , from $\lambda 1466$ and its laboratory f -value. The b -value was set at 2 km s^{-1} , as was found for Ni II, another dominant ion (Zsargó & Federman 1998). The resulting theoretical curve of growth, with $N = 8.98 \times 10^{12} \text{ cm}^{-2}$, was used to adjust the f -values of the lines at 144.801 and 148.096 nm (see Zsargó & Federman 1998). The f -value inferred from the interstellar data for the line at 148.096 nm is $0.0140_{-0.0059}^{+0.0034}$, a value that agrees nicely with our laboratory determination of 0.0119 ± 0.0010 . The good correspondence between the astronomical and laboratory results for this line provides the foundation for including an astronomical f -value for $\lambda 1448$ in Table 2. The uncertainties in the astronomical f -values include the errors in W_λ and in $f(\lambda_{\text{vac}} = 146.621)$, taken in quadrature.

Lines of interstellar Co II are also present in our spectra of ζ Oph. In particular, Federman et al. (1993) detected the line at 146.621 nm. Our f -values can be used to obtain the cobalt abundance in both cold and warm gas toward this star. The values of W_λ appear in Table 3; the resulting column densities are $N(-15) = 8.4 \times 10^{11} \text{ cm}^{-2}$ and $N(-27) = 5.8 \times 10^{11} \text{ cm}^{-2}$, where the -27 km s^{-1} com-

TABLE 3
ASTRONOMICAL RESULTS FOR INTERSTELLAR CO II.

WAVELENGTH (nm)	W_λ (mÅ)		
	ρ Oph A	ζ Oph, -15 km s^{-1}	ζ Oph, -27 km s^{-1}
148.096	$1.29 \pm 0.30(\text{stat.})_{-0.30}^{+0.00}(\text{sys.})$
146.621	$4.72 \pm 0.28(\text{stat.})_{-0.80}^{+0.10}(\text{sys.})$	0.49 ± 0.12^a	0.34 ± 0.12^a
144.801	$1.30 \pm 0.37(\text{stat.})_{-0.90}^{+0.00}(\text{sys.})$

^a From Federman et al. (1993).

ponent is warm material. These column densities translate into cobalt abundances with the use of the total hydrogen column densities derived by Savage, Cardelli, & Sofia (1992): $N_{\text{H}}(-15) = 1.32 \times 10^{21} \text{ cm}^{-2}$ and $N_{\text{H}}(-27) \sim 5.5 \times 10^{19} \text{ cm}^{-2}$. The interstellar abundances for Co II are 6.4×10^{-10} and 1.1×10^{-8} for the cold and warm gas toward ζ Oph. These abundances are about a factor of 4 larger than those quoted in Federman et al. (1993), because the refined f -values are correspondingly smaller. (Since the lines are so weak, the relative abundance between cold and warm gas has not changed.) With a solar abundance for cobalt of 8.32×10^{-8} (Anders & Grevesse 1989), the logarithmic depletions for the two parcels of gas become -2.11 and -0.88 . The refined depletions make the correspondence between depletion and condensation temperature—such as that shown in Figure 2 of Federman et al. (1993)—less clear, because cobalt is one of the most refractory elements. In any event, since the logarithmic depletion for cobalt in the warm gas is approximately -1 , an appreciable amount of cobalt (about 90%) is tied to grain material in the environment most susceptible to grain destruction.

The column density of cobalt toward ρ Oph A can be converted into an abundance by using the total column of hydrogen along the sight line— $N_{\text{H}} = 5.0 \times 10^{21} \text{ cm}^{-2}$ (Savage et al. 1977; Diplas & Savage 1994). The result is 1.8×10^{-9} , which translates into a logarithmic depletion of -1.66 . The level of depletion is less than what is deduced for the cold gas toward ζ Oph. This comparison is not

unexpected, because a larger fraction of the sight line toward ρ Oph A is cold *atomic* gas. In other words, since the fraction of hydrogen in molecular form is lower toward ρ Oph A, the amount of depletion should be less (Cardelli 1994).

5. CONCLUSION

We present absolute VUV oscillator strengths for 11 transitions arising from the ground term of Co II. Ten of these measurements were made with the High-Sensitivity Absorption Spectroscopy Experiment at the University of Wisconsin, with a typical accuracy of 10%. The laboratory method described here is applicable to essentially all elements of the periodic table, both neutral and singly ionized species, over a wide range of wavelength and line strengths. Interstellar spectra provide an additional f -value, whose absolute value is set by the laboratory data. The combined set of f -values yields refined measures of cobalt abundance and depletion in interstellar space. Future studies utilizing our f -values can elucidate the processes affecting grain evolution in a more secure manner.

This research is supported by NASA under grants NAGW-2908 and NAG5-4259 to the University of Wisconsin at Madison, by NASA grant NAGW-3840 to the University of Toledo, by STScI grant GO-05389.02-93A to the University of Toledo, and by the NSF under grant DMR-95-31009 to the Synchrotron Radiation Center.

REFERENCES

- Anders, E., & Grevesse, N. 1989, *Geochim. Cosmochim. Acta*, 53, 197
 Bergeson, S. D., Mullman, K. L., & Lawler, J. E. 1996, *ApJ*, 464, 1050
 Cardelli, J. A. 1994, *Science*, 265, 209
 Diplas, A., & Savage, B. D. 1994, *ApJS*, 93, 211
 Federman, S. R., Sheffer, Y., Lambert, D. L., & Gilliland, R. L. 1993, *ApJ*, 413, L51
 Iglesias, L. 1979, *Opt. Pura Aplicada*, 12, 63
 Kurucz, R. L. 1988, *IAU Symp.* 13, *Semiempirical Calculations of gf Values for the Iron Group*, ed. D. McNally (Kluwer: London), 168
 Mennigan, K. L., Childs, M. A., Toyoda, H., Ueda, Y., Anderson, L. W., & Lawler, J. E. 1995, *Contrib. Plasma Phys.*, 35, 359
 Morton, D. C. 1991, *ApJS*, 77, 119
 Mullman, K. L., Cooper, J. C., & Lawler, J. E. 1998, *ApJ*, 495, 503
 Pickering, J. C., Raassen, A. J. J., Uylings, P. H. M., & Johansson, S. 1998, *ApJS*, 117, in press
 Raassen, A. J. J., Pickering, J. C., & Uylings, P. H. M. 1998, *A&A*, submitted
 Savage, B. D., Bohlin, R. C., Drake, J. F., & Budich, W. 1977, *ApJ*, 216, 291
 Savage, B. D., Cardelli, J. A., & Sofia, U. J. 1992, *ApJ*, 401, 706
 Shull, J. M. 1993, *Phys. Scr.*, T47, 165
 Sugar, J., & Corliss, C. 1985, *J. Phys. Chem. Ref. Data* 14(2), 522
 Wamsley, R. C., Mitsuhashi, K., & Lawler, J. E. 1993, *Rev. Sci. Instrum.*, 64, 45
 Zsargó, J., & Federman, S. R. 1998, *ApJ*, 498, in press
 Zsargó, J., Federman, S. R., & Cardelli, J. A. 1997, *ApJ*, 484, 820